Polyarginine as a Simultaneous Antimicrobial, Immunomodulatory, and miRNA Delivery Agent within Polyanionic Hydrogel

Varvara Gribova, Lauriane Petit, Leyla Kocgozlu, Cendrine Seguin, Sylvie Fournel, Antoine Kichler, Nihal Engin Vrana, Philippe Lavalle

Polyarginine as a simultaneous antimicrobial, immunomodulatory and miRNA delivery agent within polyanionic hydrogels

*Varvara Gribova, Lauriane Petit, Cendrine Seguin, Sylvie Fournel, Antoine Kichler, Nihal Engin Vrana, Philippe Lavalle**

*Corresponding author

V. Gribova, L. Petit, P. Lavalle

Institut National de la Santé et de la Recherche Médicale, Inserm UMR_S 1121 Biomaterials and Bioengineering, Strasbourg, France

Université de Strasbourg, Faculté de Chirurgie Dentaire, Strasbourg, France

C. Seguin, S. Fournel, A. Kichler

Université de Strasbourg, CNRS, 3Bio team, Laboratoire de Conception et Application de Molécules Bioactives, UMR 7199, Faculté de Pharmacie, Illkirch, France

N. E. Vrana, P. Lavalle

SPARTHA Medical, Strasbourg, France

E-mail: philippe.lavalle@inserm.fr

Keywords: biomaterials, hydrogels, antibacterial, anti-inflammatory, miRNA

Abstract

Implantation of biomedical devices is followed by immune response to the implant, as well as occasionally bacterial, yeast and/or fungal infections. In this context, new implant materials and coatings that deal with medical device-associated complications are required. Antibacterial and anti-inflammatory materials are also required for wound healing applications, especially in diabetic patients with chronic wounds. In this work, we present hyaluronic acid (HA) hydrogels with triple activity: antimicrobial, immunomodulatory and miRNA delivery agent. We demonstrate that polyarginine with a degree of polymerization of 30 (PAR30), which was previously shown to have a prolonged antibacterial activity, decreases inflammatory response of LPS-stimulated macrophages. In addition, PAR30 accelerated fibroblast migration in macrophage/fibroblast co-culture system, suggesting a positive effect on wound healing. Furthermore, PAR30 allowed to load miRNA into HA hydrogels, and then to deliver them into the cells. To our knowledge, this study is the first describing miRNA-loaded hydrogels with antibacterial effect and anti-inflammatory features. Such system is promising for the treatment of infected wounds, e.g. diabetic ulcers, as well as for foreign body response modulation.

Introduction

The number of implants and prostheses used to treat various medical conditions increases every year. Implantation of biomedical devices is followed by immune response to the implant, but also occasionally bacterial, yeast and/or fungal infections.[1-3] Among healthcare-associated infections, nearly 50% can be attributed to medical devices.[4] Mortality due to these infections depends on the type of device and can range from less than 5% for dental implants to impressive 25% for heart valves.[5]

Although some of the infections can be successfully treated with antibiotics, bacterial antibioresistance, leads to extended illness duration, increasing treatment costs and higher mortality rates. This growing problem has been declared by World Health Organization as one of 10 biggest threats to global health.[6] In this context, new implant materials and coatings that can decrease medical device-associated complications due to infection have to be developed.[7-9]

Even in the absence of bacterial infection, excessive inflammation, which may occur as a response to implantation, is another serious issue. An uncontrolled, chronic inflammation can induce implant's degradation and collateral damages to surrounding tissues, as well as a fibrotic capsule formation, leading to implant's failure.[1] Materials trying to overcome this problem, and more particularly inducing macrophage differentiation into M2 (pro-resolving) instead of M1 (pro-inflammatory) phenotype are also under development (for review, see Lebaudy et al., 2021[10]).

Antibacterial and anti-inflammatory materials are also required for wound healing applications, especially in diabetic patients with chronic infected wounds.[11] In addition, such wounds are associated with high levels of pro-inflammatory cytokine secretion and iNOS production, contributing to non-healing phenotype.[12]

Hyaluronic acid (HA) is a component of the ECM which is biocompatible and used for multiple biomedical applications: osteoarthritis treatment, dermal injections, eye surgery, and wound regeneration.[13] HA is an extremely versatile molecule that can provide multiple functionalities. We have previously described thin films made of HA and polyarginine (PAR). Such films constructed by layer-by-layer assembly demonstrated antimicrobial and anti-inflammatory properties. [14-16] Recently, we presented antibacterial HA-based hydrogels cross-linked with 1,4-butanediol diglycidyl ether (BDDE).[17] One of the advantages of using this cross-linker is that BDDE is already used to stabilize HA in injectable hydrogels for cosmetic purposes.[18] In addition, in HA hydrogels cross-linked with BDDE, carboxylic groups are preserved, and can be used for complexation with positively-charged antibacterial polymers such as PAR.[15-16] The results demonstrated a strong antibacterial activity of PAR-loaded HA hydrogels, with polyarginine having 30 arginine residues, PAR30, providing the best long-term antibacterial effect. Moreover, first animal experiments were performed and showed good biocompatibility of HA/PAR hydrogels *in vivo.*[17] PAR has also been described as a possible vector for nucleic acid delivery.[19-20]

Among nucleic acids, micro-RNA (miRNA) are small non-coding RNAs that regulate post-transcriptional gene expression. They present the advantage of an easy production and are already in clinical trials to treat hepatitis, polycystic kidney disease or cancer.[21-22] In the biomaterials field, only few hydrogel systems for miRNA delivery were described: gelatin-PEG gels for osteogenesis,[23] gelatin hydrogel loaded with HA-miRNA nanoparticles for immunomodulation,[24] miRNA plasmid/nanoparticles in HA hydrogel for tendon healing,[25] and injectable miRNA functionalized hydrogel for cardiomyocyte regeneration.[26]

However, none of these systems have a safety measure for potential infections. In the present work, we demonstrate that in addition to its antibacterial properties, PAR30 decreases inflammatory response in LPS-stimulated murine macrophages. We also show its ability to

form complexes with negatively-charged miRNA to load them into polyanionic HA hydrogels, and then deliver them into Balb3T3 fibroblastic cells.

To our knowledge, the study presented in this paper is the first describing miRNA-loaded hydrogels with antibacterial effect and anti-inflammatory features. Such system is promising for the treatment of infected wounds, e.g. diabetic ulcers. **(Figure 1).**

T

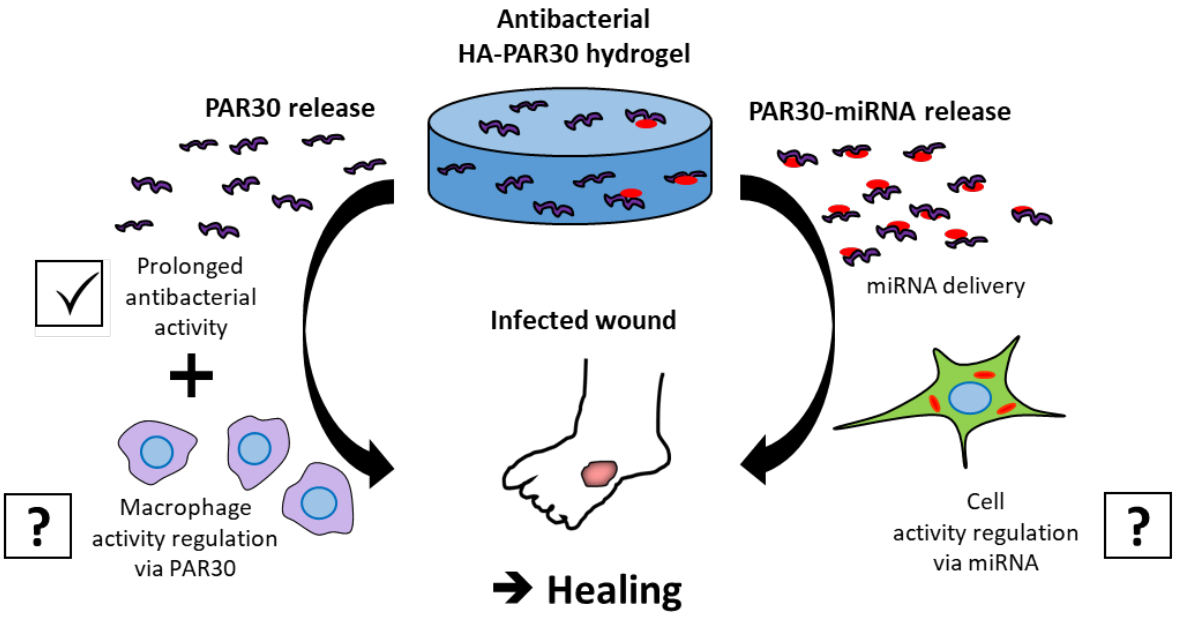

Figure 1. Experimental design of HA/PAR30/miRNA hydrogels with triple antibacterial, immunomodulatory and miRNA-delivering activities. Such hydrogels are designed for potential applications such as wound healing, particularly for diabetic infected skin ulcers.

Materials and methods

Materials

Poly(L-arginine hydrochloride) (PAR30, MW = 5.8 kDa) was purchased from Alamanda Polymers, USA. Hyaluronic acid (HA, MW = 823 kDa) used as the polyanion was purchased from Lifecore Biomed (USA). Tris(hydroxymethyl)-aminomethane (Tris), butanediol diglycidyl ether (BDDE), lipopolysaccharide (LPS) and Mueller Hinton broth medium (MH) were purchased from Merck (Germany). High glucose *DMEM (Dulbecco's Modified Eagle Medium*), 100x penicillin-streptomycin and ultra-low endotoxin fetal bovine serum (FBS) were purchased from Dominique Dutscher (France). RNeasy Plus Micro Kit was purchased from Qiagen, and all the reagents for qRT-PCR, as well as non-labeled miRNAs and Alamar Blue reagent were purchased from Life Technologies / Thermo Fisher (France). INTERFERin was purchased from Polyplus-transfection (France). miRIDIAN microRNA Mimic Transfection Control with Dy547 was purchased from Horizon Discovery (UK). All antibodies, phalloidin-FITC and IL-4 were purchased from Abcam, and DAPI was purchased from Cell Signaling Technology.

Cell culture

RAW 264.7 murine macrophages (ATCC TIB71) and Balb/3T3 (ATCC CCL163) mouse embryonic fibroblast cell line were cultured at 37°C in *DMEM* with 5% of low endotoxin FBS and 1% of penicillin-streptomycin (further referred to as “DMEM-FBS”). The cells were passaged 2-3 times a week and used at passages 5-20 (RAW 264.7) and 10-30 (Balb/3T3). For M1 or M2 induction controls, RAW 264.7 macrophages were treated with 100 ng/mL LPS and 10 ng/mL IL-4, respectively.

Cell viability test

Cell viability was evaluated by Alamar Blue assay in a 24-well plate on $2x10^4$ of RAW 264.7 macrophages and 10^5 of Balb3T3 fibroblasts. After 24h at 37°C, the cells were treated with PAR30/miRNA in solution or from the hydrogel, and the cells were incubated for another 24h. Then, Alamar Blue test was performed according to manufacturer's instructions. Briefly, Alamar Blue reagent was diluted at 1/10 in DMEM-FBS medium and added to the cells. After 3 hours of incubation at 37°C, medium fluorescence at 560/590 nm (ex/em) was measured in black 96-well plates. All the conditions were performed in triplicate.

NO quantification

NO secretion was measured using Griess-Saville method. For this, 5 x 10^5 of RAW 264.7 cells were seeded into 24-well plate for 24h. After 24h of treatment with controls/PAR30/miRNA, 100 µL of the supernatants were transferred into 96-well plate, and 100 µL of 10% (v/v) of acetic acid (pH 2.5) were added. Then, 40 µL of sulfanilamide 6 mg/mL were added, and the plate was incubated for 3 min at RT under agitation. Finally, 10 µL of N-(1-naphtyl)ethylenediamine (NED) were added, and the plate was incubated for 5 min at RT under agitation. The absorbance at 570 nm was measured using Safas Genius XC spectrofluorimeter (Monaco). In parallel, the cells were fixed and stained with DAPI for cell number evaluation. The results are presented as averages of absorbance at 570 nm divided by the cell number and normalized to the control (untreated cells).

qRT-PCR

For qRT-PCR experiments, 10^5 of RAW 264.7 cells were seeded into 24-well plate for 24h. After 24h of treatment with controls/PAR30/miRNA, the cell culture medium was discarded and 100 µL of RNAlater were added. The bottom of the wells was then scratched

with a pipet tip, and the lysates were stored at +4°C for 2 days, then at -20°C. RNA purification was performed using RNeasy Plus Micro Kit, and reverse transcription was done on 0.5 µg total RNA using SuperScript IV VILO Master Mix with ezDNase Enzyme, according to manufacturer's instructions. For quantitative PCR, TaqMan Fast Advanced Master Mix was used with TaqMan Gene Expression Assays **(Table 1).** The results were analysed by $2^{-(\Delta\Delta Ct)}$ method: iNOS mRNA expression is relative to Gapdh and control, non-stimulated cells.

Table 1. List of TaqMan Gene Expression Assays used in the study.

Gene name	Assay ID (ThermoFisher)
Gapdh	Mm99999915_g1
Nos2	Mm00440502_m1

Immunofluorescent labelling

For fluorescence experiments, 5 x 10^4 of RAW 264.7 cells were seeded into 24-well plate for 24h. After 1-3 days of treatment with controls/PAR30/miRNA, the cells were fixed with 4% paraformaldehyde (PFA) in PBS for 15 min at room temperature. Cell morphology was observed after cell staining with phalloidin-FITC (1/1000) and 5 µg.mL^{-1} DAPI, both diluted at in PBS and incubated for 10 min at room temperature. For M1 and M2 marker labelling, the cells were washed 3 times in PBS containing 0.1% Triton-X and blocked with 10% FBS in PBS for 30 min. Primary antibodies were mouse monoclonal anti-iNOS antibody [NOS-IN] (ab49999) and rabbit polyclonal anti-mannose receptor (CD206) antibody (ab64693), both diluted at 1/100. Secondary antibodies were goat anti-mouse Alexa Fluor® 647-conjugated antibody (ab150115) and goat anti-rabbit Alexa Fluor® 488-conjugated antibody (ab150077), both diluted at 1/200. Primary and secondary antibodies were incubated with the cells for 1h at

room temperature, following by 3 PBS rinses. The cells were observed using Zeiss LSM710 confocal microscope.

Hydrogel construction

HA hydrogels were prepared according to previously published procedure.[17] Briefly, 1.5 mL of 2.5% HA (MW = 823 kDa) solution in NaOH (0.25 M) was mixed with 20% BDDE (v/v) and poured into a 35-mm diameter Petri dish. The mixture was allowed to cross-link at room temperature for 72 hours. The hydrogel was further cut when necessary into 4-mm discs using a circle cutter and rinsed in Tris 10 mM /NaCl 0.15 M buffer (further referred to as Tris/NaCl buffer). An initial 1 min rinsing and a longer 1-hour rinsing were performed. After this procedure, 4 mm diameter discs have swollen and became 6 mm diameter discs.

Loading and release of PAR/miRNA

The discs were immersed in 100 $\mu g.mL^{-1}$ PAR30-FITC (produced in the laboratory as described in[15]) and 60 nM of miRNA-Dy547 solution in Tris/NaCl buffer and incubated for 24h at room temperature on a moving plate. For 6 mm discs in 24-well plate, 0.5 mL of PAR30/miRNA solution was used. After incubation, the discs were rinsed with Tris/NaCl buffer (one quick and one long rinsing, 5 min and 1 hour, respectively).

For release experiments, discs were incubated at 37°C with respective solution (Tris/NaCl buffer, MH bacterial culture medium or DMEM supplemented with 5% FBS and 1% antibiotics). The release quantification was performed using confocal laser scanning microscopy (Zeiss LSM 710, Heidelberg, Germany) and ImajeJ software.

Transfection

Prior to transfection, 10^5 of Balb3T3 fibroblasts were seeded in 24-well plates for 24 hours in 1 mL of DMEM-FBS medium. For transfection in solution, 550 µL of medium were discarded from the well. PAR30/miRNA 10x transfection mix was prepared in serum-free DMEM medium. After 15 minutes of incubation at room temperature, 50 µL of the mix was added to 450 µL of the DMEM-FBS medium remaining in the wells and incubated at 37°C for the desired time. For transfection from the hydrogel, HA/PAR30/miRNA hydrogels were prepared as described above (see "Loading and release of PAR/miRNA") and placed into the well containing the cells. The imaging was performed using confocal laser scanning microscopy (Zeiss LSM 710, Heidelberg, Germany).

Microbiology assays

Staphylococcus aureus (ATCC 25923) strain was used to assess the antibacterial properties of the test samples. Bacterial strain was pre-cultured aerobically at 37°C in a Mueller Hinton broth (MH) medium, pH 7.3. For this, one colony from previously prepared agar plate with streaked bacteria was transferred to 10 mL of MH medium and incubated at 37°C. Overnight culture was adjusted to $OD_{620\,nm} = 0.001$ (approximately $8x10^5$ CFU/mL) by diluting in MH, and added to the wells of a 24-well plate containing d = 6 mm HA hydrogels loaded with 100 $\mu g.mL^{-1}$ PAR30 and 60 nM of miRNA-Dy547 (or 6 µL of INTERFERin per 500 µL pre-incubated with 60 nM of miRNA-Dy547 as a control) and sterilized with UV for 15 min. Antibacterial effect of the hydrogels was quantified by measuring $OD_{620\ nm}$ after 24h of incubation at 37°C on a moving plate.

Statistical Analysis

Each experiment was performed at least three times, if not specified otherwise. Either representative results or averages from three independent experiments are shown in the Figures. Error bars correspond to standard deviation. The data were processed by using SigmaPlot (Systat Software Inc., USA). Student's t-test or one-way ANOVA on Ranks were performed to evaluate statistical significance.

Results and Discussion

1. PAR30 decreases inflammatory response in macrophages

Tissue resident macrophages, as well as monocyte-derived macrophages, are one of the most important actors of inflammation.[27] Successful biomaterials implantation requires a slight equilibrium between "necessary" and deleterious inflammation in response of biomaterials. Thus, new biomaterials such as PAR30-loaded hydrogels have to be tested for their inflammatory properties. In this study, we used LPS-treated RAW 264.7 cells to assess anti-inflammatory properties of PAR30, which was used as an antibacterial agent loaded into HA hydrogels in our previous study.[17]

RAW264.7 cells is a murine macrophage cell line widely described as *in vitro* model to study inflammation. RAW264.7 could easily be activated by part of bacterial wall, namely lipopolysaccharide (LPS). The LPS pro-inflammatory signals induce cell shape modification, production of nitric oxide (NO) and cytokine secretion. NO is produced by macrophages following inducible NO synthase (iNOS) production.[28]

Polycations at high concentrations can show toxicity due to their interaction with the negatively-charged cell membrane. Using active mitochondrial metabolism as viability marker (Alamar Blue assay), a non-toxic concentration of 10 µg/mL of PAR30 was determined and used for the rest of the studies on RAW264.7 cells **(Figure S1)**.

To evaluate PAR-30 anti-inflammatory effect, NO secretion (Griess-Saville assay; Figure 2A) and iNOS mRNA synthesis induction (qRT-PCR; Figure 2B) in LPS-treated macrophages were followed, and showed significant reduction in presence of PAR30. All together, these results suggest that PAR30 have an anti-inflammatory effect. Previous studies of our group using primary human macrophages and showing that PAR/HA multilayer did not induce pro-inflammatory cytokine production (TNFα) even in IFNγ-activated macrophages, are in agreement with this anti-inflammatory effect.[14]

Macrophage polarization leads to M1 (pro-inflammatory) macrophage phenotype or M2 anti-inflammatory and pro-resolving macrophages. We evaluated the effect of PAR30 on macrophage polarization. M2 marker CD206 was used to label macrophages M2 and iNOS to label M1 macrophages. As expected, LPS induced strong iNOS expression, while IL-4, which allows macrophage differentiation into M2 phenotype, induced CD206 expression. PAR30 treatment, with or without LPS stimulation, did not induce iNOS expression, while CD206 staining was present, indicating macrophage orientation towards M2 phenotype. Since LPS is a powerful M1 inductor, such a counteracting effect by PAR30 can be highly useful to decrease chronic inflammations related to implants and wound settings.

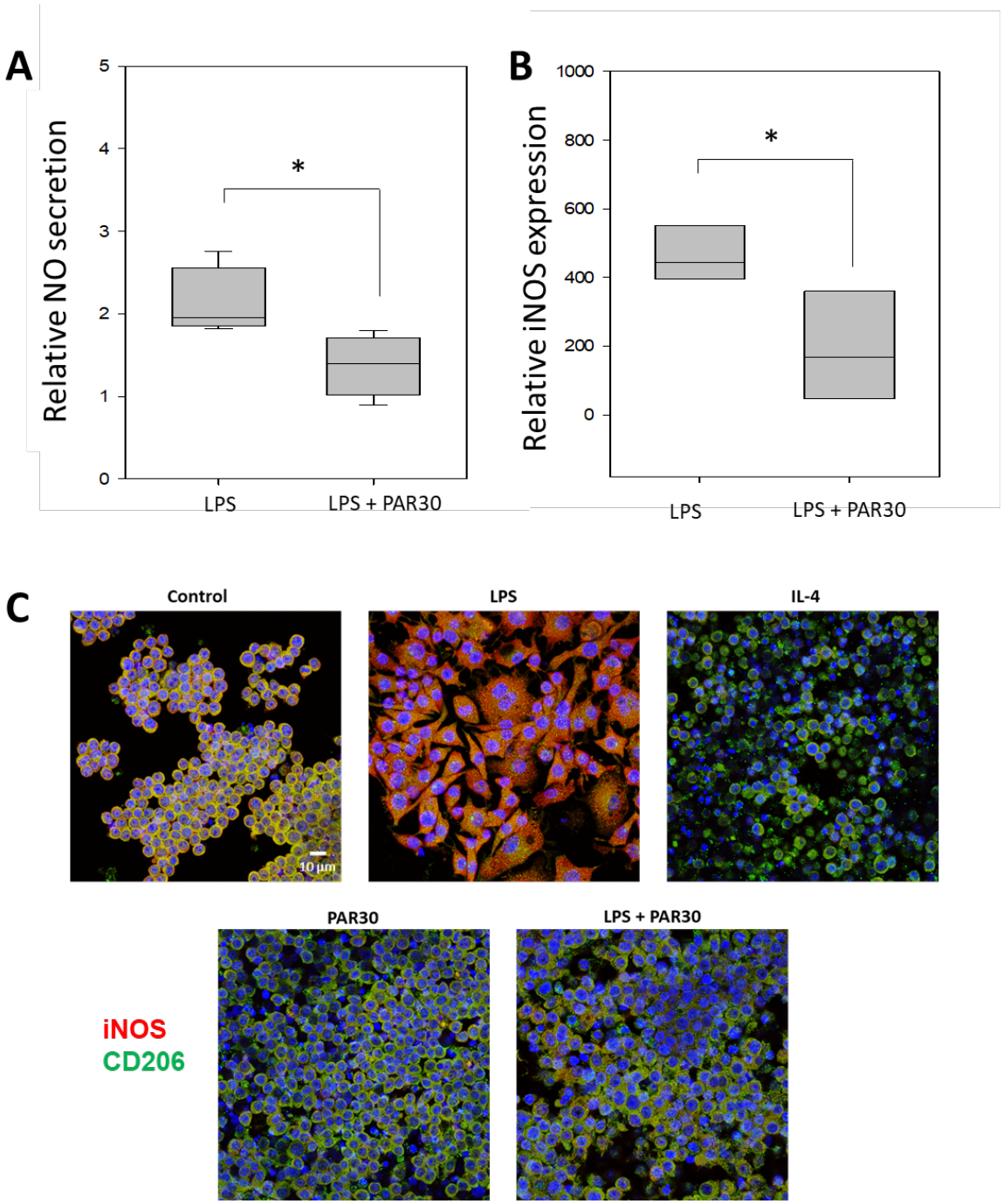

Figure 2. Effect of PAR30 on LPS-induced inflammatory response in RAW264.7 macrophages. (A) PAR30 decreases NO secretion (Griess assay, n = 4) and **(B)** iNOS mRNA expression (qRT-PCR, n = 3) after 24h treatment in LPS-treated macrophages. Griess results are presented as OD 570 nm averages divided by the cell number (DAPI staining used for the quantification not shown) and normalized to the control (untreated cells). iNOS mRNA expression is relative to Gapdh and control, non-stimulated cells according to $2^{-\Delta\Delta Ct}$ analysis method**. (C)** RAW264.7 are treated for 72h with 100ng/mL LPS or IL4 before fixation and staining of iNOS (red), CD206 (green) and nuclei (blue). Representative results of three independent experiments are shown. Scale bar corresponds to 10 µm.

One of the important stages in the resolution phase of inflammatory response is fibroblast recruitment and migration to the inflammation site. Fibroblast respond to paracrine factors secreted by macrophages, in particular, shifting from inflammation-related activity to the synthesis of new ECM components for tissue regeneration.[29] To study the effect of PAR30 on fibroblast migration, we used a macrophage-fibroblast co-culture system using Ibidi® chambers. Briefly, the macrophages were treated with LPS and LPS + PAR30, then the chamber was removed to allow macrophage-fibroblast communication **(Figure 3A)**. The results show that the gap closure time between fibroblasts decreased about 1.5 times upon PAR30 stimulation of macrophages **(Figure 3B)**. In addition, fibroblast morphology changed significantly in presence of PAR30-stimulated macrophages **(Figure S2A)**. Thus, cell area decreased, while aspect ratio increased, as quantified from the images **(Figure S2B).** Aspect ratio is the ratio of width to height, and is used to characterize cell elongation.

Interestingly, macrophage migration was affected as well, since more macrophages were detected among fibroblasts in control and LPS + PAR30 conditions, as compared to LPS **(Figure S3)**. These results show, for the first time, the indirect effect of PAR30 on fibroblast migration, which correlates with cell morphology modification and presence of macrophages among fibroblasts. These changes are probably due to different molecule secretion (such as cytokines, chemokines etc.) by macrophages and/or fibroblasts under given experimental conditions. Studies to better characterize this phenomenon are ongoing.

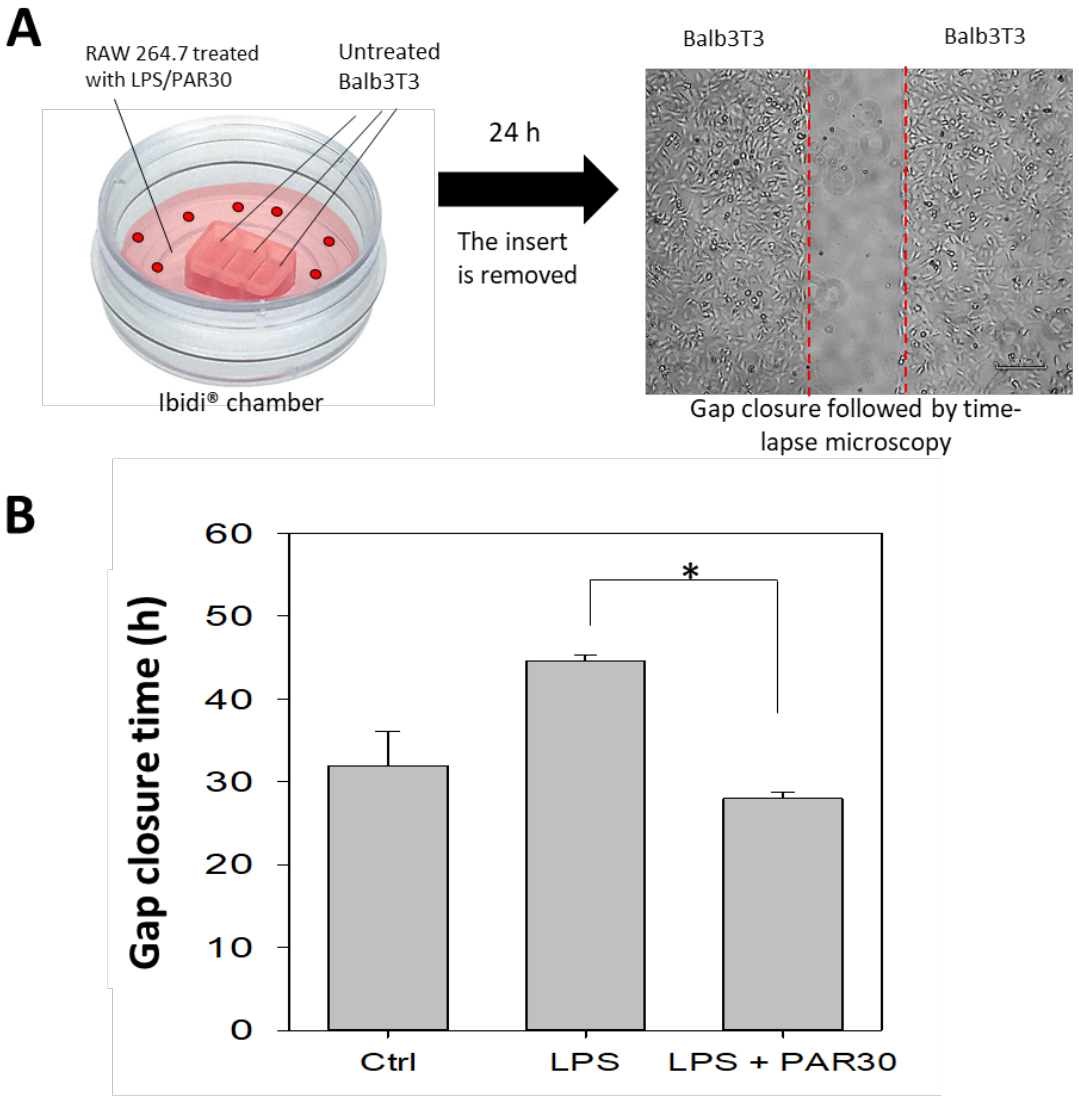

Figure 3. PAR30-treated macrophages accelerate fibroblast migration. (A) Experimental design: 5 x 10^4 RAW 264.7 macrophages seeded in 1 mL of cell culture medium were treated with 100 ng.mL^{-1} LPS and 10 µg.mL^{-1} PAR30 for 24 hours, before insert removal. Fibroblast (seeded at 5 x 10^3 cells per chamber well) migration was followed using time-lapse microscopy. **(B)** Gap closure time between Balb3T3 fibroblasts in presence of macrophages. *$p<0.05$

2. PAR30 is an efficient vector for miRNA delivery

The second hypothesis in our study concerned the ability of PAR30 to act as a carrier for nucleic acids loading into negatively charged hydrogels and to deliver these nucleic acids into the cells. Polycationic molecules are well-known for their ability to form complexes with negatively charged nucleic acids, and interact with cell membranes to deliver nucleic acids into the cells. Polyethyleneimine (PEI) is probably the most well-known of them, however with significant cytotoxicity.[28] Polyarginine has also been previously used to deliver nucleic acids into the cells.[16] However, to our knowledge, only few studies reported the use of polyarginine peptides (made of 9 and 11 units of arginine) for miRNA delivery.[29-30]

First, we evaluated the capacity of the PAR30 to form complexes the miRNA. To this end, a gel mobility shift assay was done using increasing amounts of polyarginine mixed with a constant amount of miRNA. Results showed that approximately 2 μg PAR30/0.8 μg miRNA were required for complete retardation **(Figure S4)**. Next, we investigated if these complexes can be loaded into a negatively-charged HA hydrogels described in our previous study.[17] When hydrogel discs were incubated with control fluorescent miRNA alone, no miRNA penetrated inside the hydrogel, as shown in **Figure 4A**. However, when miRNA was pre-incubated with PAR30 (100 $\mu g.mL^{-1}$ PAR30 with 60 nM miRNA), fluorescence could be detected inside the hydrogel **(Figure 4A)**, showing that PAR30-miRNA complexes are efficiently loaded in the hydrogel.

We then evaluated if PAR30-FITC and miRNA-Dy547 were released from the hydrogels in Tris/NaCl buffer, as well as in DMEM and MH media (macrophage and bacterial culture media, respectively). After 24h at 37°C in Tris/NaCl buffer, PAR30 remained in the hydrogel, confirming our previous results,[17] while some decrease in miRNA was also observed **(Figure 4B and C).** In DMEM and MH, only small quantities of both PAR30 and miRNA remained in the hydrogels after 24h, showing efficient PAR30 and miRNA release from the

hydrogels. Such difference of the release in Tris/NaCl buffer versus DMEM and MH is probably due to the presence of various molecules such as proteins and sugars in cell culture media, which destabilize PAR30 interaction with HA.

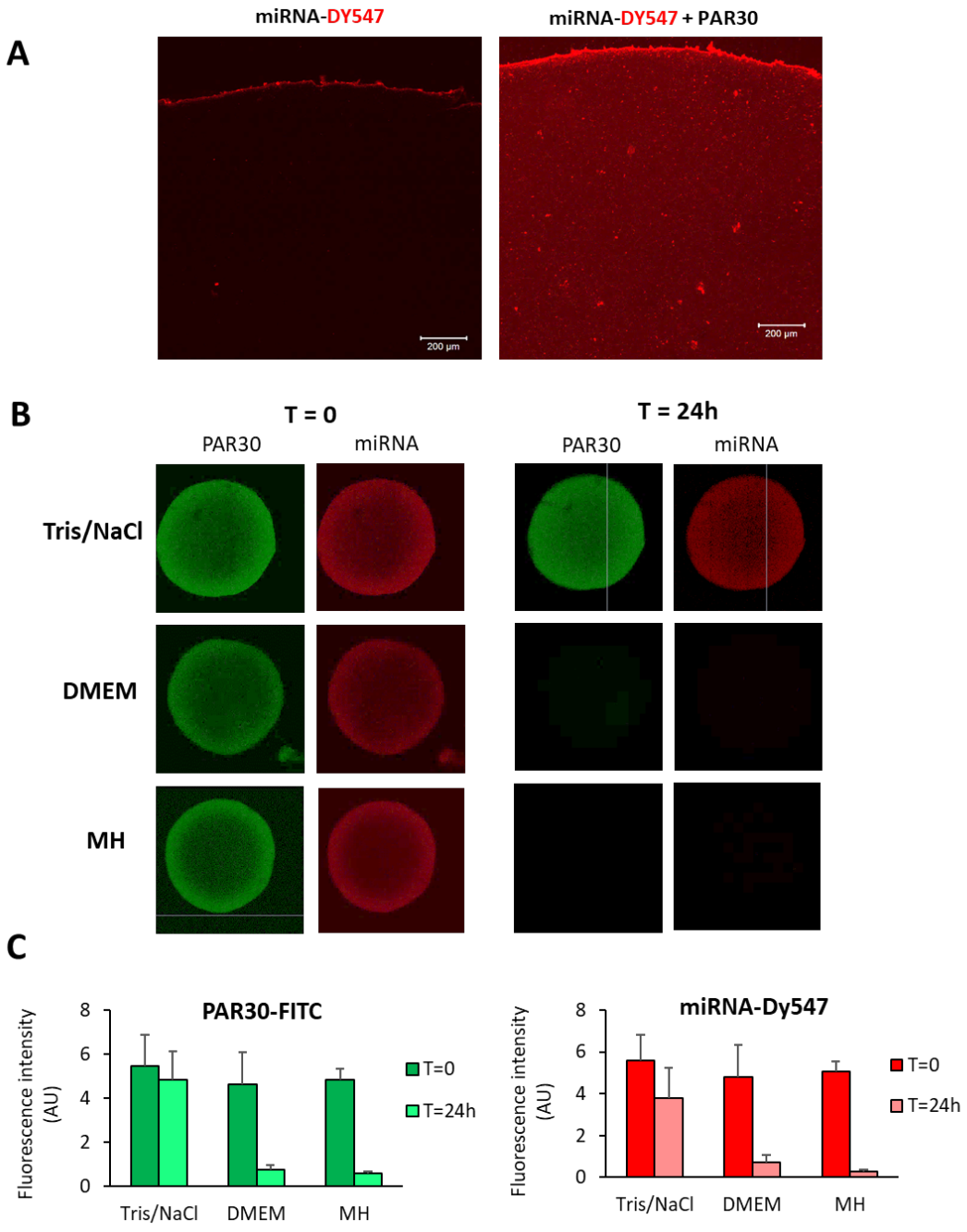

Figure 4. PAR30/miRNA loading and release into/from HA hydrogels. (A) miRNA loading into the hydrogels with or without PAR30 in Tris/NaCl buffer. **(B)** and **(C)** miRNA-Dy547 (red) and PAR30-FITC (green) release kinetics according to media. Representative results of 2 independent experiments are shown. The bars correspond to fluorescence averages quantified from 3 images, and the error bars represent standard deviation.

Finally, PAR30/miRNA-loaded HA hydrogels were placed in the wells containing Balb3T3 fibroblasts, and cell transfection was evaluated **(Figure 5A)**. As a control, PAR30/miRNA in solution was used. The results showed the presence of multiple fluorescent dots in the cells treated with PAR30/miRNA in solution, and fewer dots when PAR30/miRNA was released from the hydrogels **(Figure 5B).** This decrease can be due to PAR30/miRNA complex dissociation upon release from negatively-charged hydrogels. Still, cell transfection was efficient even in these conditions, showing that HA/PAR30/miRNA hydrogels are a potential tool for miRNA delivery. We also evaluated cell viability using Alamar Blue test **(Figure 5C)**, showing some cytotoxicity (viability < 70%) of HA/PAR30/miRNA hydrogels. This is probably due to a high PAR30/miRNA concentration at the hydrogel/cell interface, which leads to a decrease of cell number in the well.

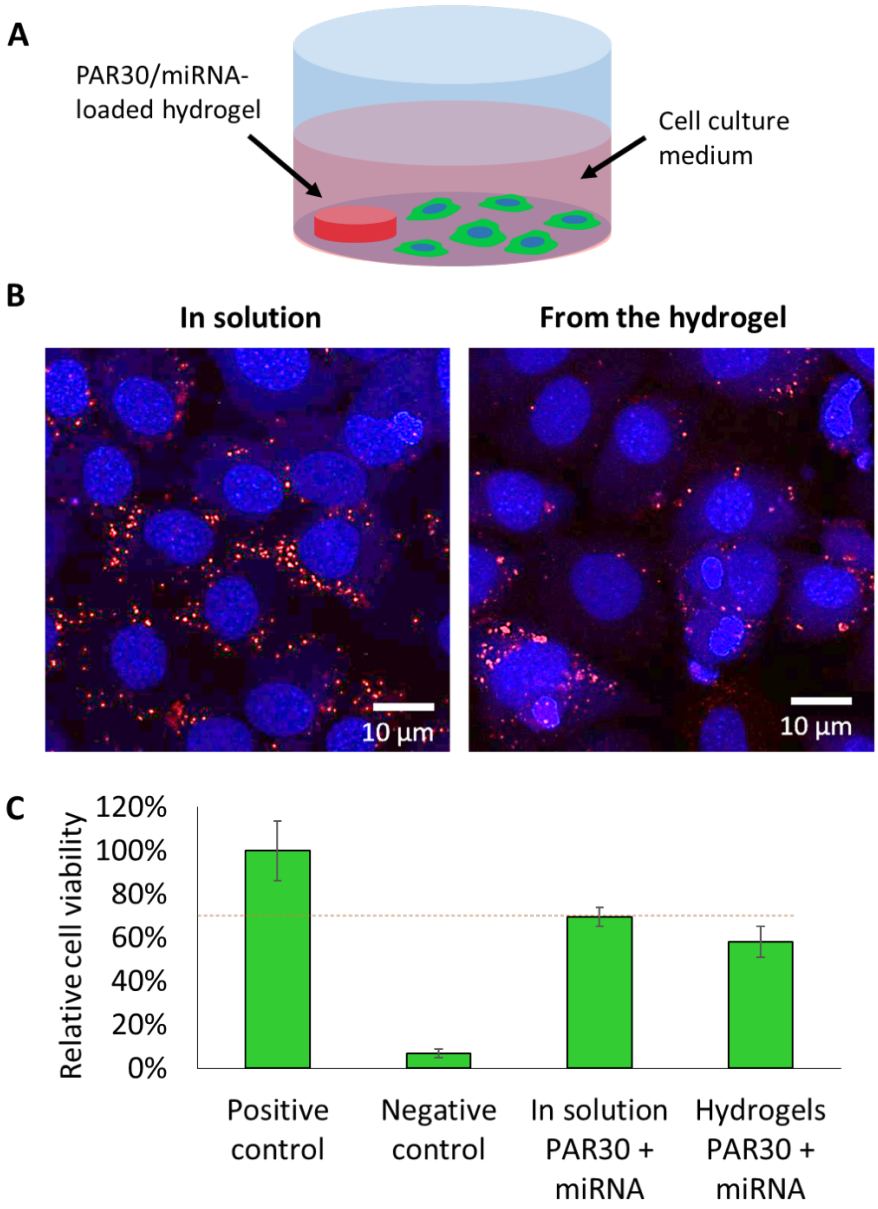

Figure 5. Cell transfection using HA/PAR30/miRNA hydrogels. (A) Schematic representation of the experiment. **(B)** Fluorescent miRNA (red) visualization in Balb3T3 fibroblasts, nuclei are labeled in blue (DAPI staining). The results are representative of 2 independent experiments. **(C)** Cell viability evaluation by Alamar Blue assay (n=1). Positive control corresponds to untreated cells, and negative control is 10% DMSO-treated cells. The results are normalized to the positive control (100% viability), the bars represent averages of 3 wells and the error bars correspond to standard deviation.

3. HA/PAR30/miRNA hydrogels preserve antibacterial activity

Antibacterial activity of HA/PAR30/miRNA system was evaluated using *Staphylococcus aureus* **(Figure 6A).** For this, bacteria were grown in the wells containing PAR30/miRNA-loaded and control hydrogels. No bacterial growth was detected after 24h in the wells containing PAR30/miRNA-loaded hydrogel, demonstrating that antibacterial activity of PAR30 is preserved in presence of miRNA **(Figure 6B)**. INTERFERin transfection agent containing cationic components was used as a control, and it didn't demonstrate any antibacterial activity at a concentration capable to transfect the cells.

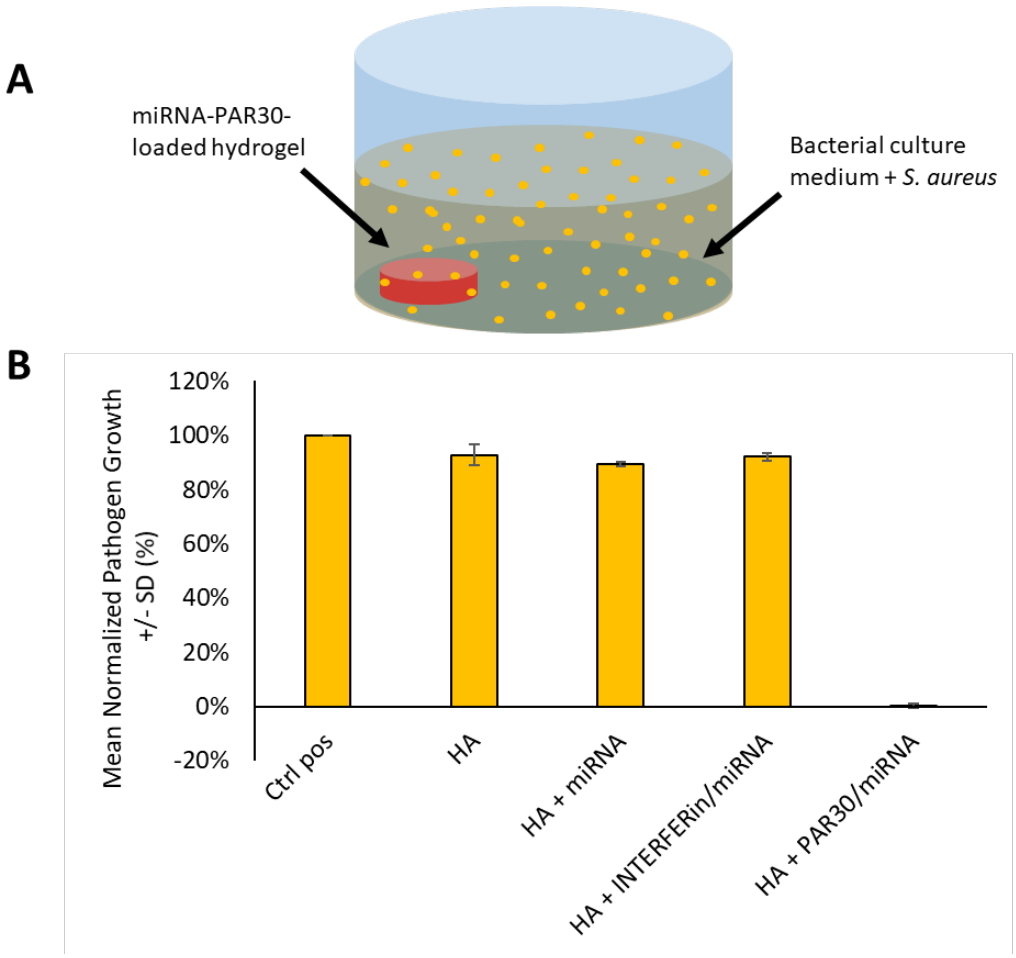

Figure 6. Antibacterial activity of PAR30/miRNA-loaded HA hydrogels. (A) Schematic representation of the assay. **(B)** Antibacterial activity evaluated on *Staphylococcus aureus*. Antibacterial effect was quantified by measuring $OD_{620\ nm}$ after 24h of incubation at 37°C on a moving plate. The bars represent averages of 2 independent experiments, error bars correspond standard deviation.

Conclusions and Perspectives

For the first time, we describe PAR30/miRNA-loaded hydrogels with antibacterial properties, which simultaneously act as miRNA delivery system **(Figure 7)**. Potentially any miRNA can be used, making the system highly versatile. For instance, the hydrogels can be associated to different functional miRNAs, such as anti-inflammatory or angiogenic, to increase anti-inflammatory properties or to induce revascularization at the wound site. In addition, we show that PAR30 possesses anti-inflammatory features, by reducing production of inflammatory markers in RAW264.7 macrophages. We believe that our system can be useful for the treatment of infected and inflamed wounds such as diabetic ulcers, that are extremely difficult to heal and usually end up with amputations.

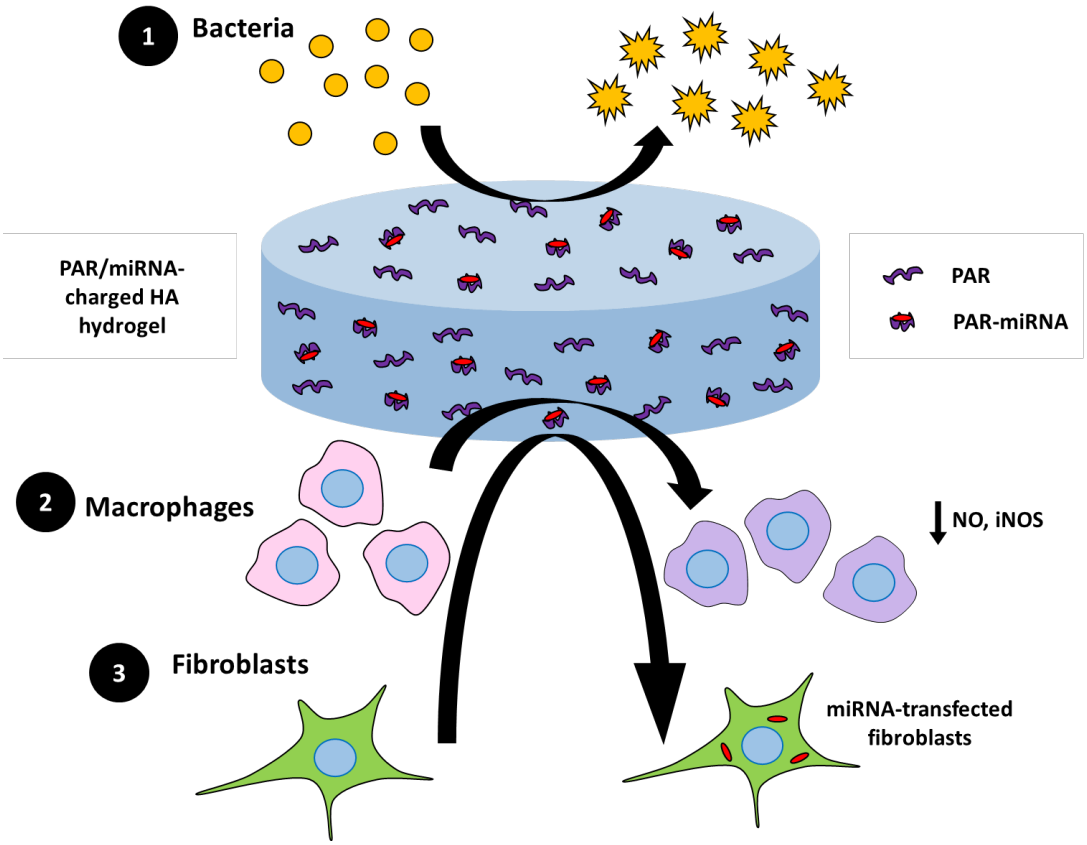

Figure 7. Schematic representation of different polyarginine activities. HA hydrogels loaded with PAR30/miRNA provide antimicrobial, immunomodulatory and miRNA delivery activities.

Author Contributions

V.G., N.E.V. and P.L. conceptualized the study, V.G., L.P. and C.S. performed the experiments and analyzed the results, V.G., S.F., A.K., N.E.V. and P.L. wrote and reviewed the manuscript.

Additional information

The following files are available: Supporting Information Figures S1-S3.

Conflicts of interest

Competing interests: N.E.V. is the majority shareholder and P.L. is CSO of SPARTHA Medical which is a coating development company. The article does not contain any information about SPARTHA products.

Acknowledgements

This project received funding from the European Union's Horizon 2020 PANBioRA research and innovation program under grant agreement no. 760921, from Bourse French Tech "Emergence grant" and from Region Grand Est through the "ERMES" project.

References

1. Morais, J. M.; Papadimitrakopoulos, F.; Burgess, D. J. Biomaterials/Tissue Interactions: Possible Solutions to Overcome Foreign Body Response. *AAPS J* **2010,** *12*, 188-196.
2. VanEpps, J. S.; Younger, J. G. Implantable Device-Related Infection. *Shock* **2016,** *46*, 597-608.
3. Shen, P.; Chen, Y.; Luo, S.; Fan, Z.; Wang, J.; Chang, J.; Deng, J. Applications of biomaterials for immunosuppression in tissue repair and regeneration. *Acta Biomater* **2021,** *126*, 31-44.
4. Darouiche, R. O. Treatment of infections associated with surgical implants. *NEJM* **2004,** *350*, 1422-9.
5. Darouiche, R. O. Device-associated infections: a macroproblem that starts with microadherence. *Clin Infect Dis* **2001,** *33*, 1567-72.
6. Laxminarayan, R.; Duse, A.; Wattal, C.; Zaidi, A. K.; Wertheim, H. F.; Sumpradit, N.; Vlieghe, E.; Hara, G. L.; Gould, I. M.; Goossens, H.; Greko, C.; So, A. D.; Bigdeli, M.; Tomson, G.; Woodhouse, W.; Ombaka, E.; Peralta, A. Q.; Qamar, F. N.; Mir, F.; Kariuki, S.; Bhutta, Z. A.; Coates, A.; Bergstrom, R.; Wright, G. D.; Brown, E. D.; Cars, O. Antibiotic resistance-the need for global solutions. *Lancet Infect Dis* **2013,** *13*, 1057-98.
7. Santos, M. R. E.; Fonseca, A. C.; Mendonça, P. V.; Branco, R.; Serra, A. C.; Morais, P. V.; Coelho, J. F. J. Recent Developments in Antimicrobial Polymers: A Review. *Materials* **2016,** *9*, 599.
8. Ergene, C.; Yasuhara, K.; Palermo, E. F. Biomimetic antimicrobial polymers: recent advances in molecular design. *Polym Chem* **2018,** *9*, 2407-2427.
9. Li, Z.; Bai, H.; Jia, S.; Yuan, H.; Gao, L.-H.; Liang, H. Design of functional polymer nanomaterials for antimicrobial therapy and combatting resistance. *Mater Chem Frontiers* **2021,** *5*, 1236-1252.
10. Lebaudy, E.; Fournel, S.; Lavalle, P.; Vrana, N. E.; Gribova, V. Recent Advances in Antiinflammatory Material Design. *Adv Healthc Mater* **2021,** *10(1)*:2001373
11. Wang, H.; Xu, Z.; Zhao, M.; Liu, G.; Wu, J. Advances of hydrogel dressings in diabetic wounds. *Biomater Sci* **2021,** *9*, 1530-1546.
12. Hesketh, M.; Sahin, K. B.; West, Z. E.; Murray, R. Z. Macrophage Phenotypes Regulate Scar Formation and Chronic Wound Healing. *Int J Mol Sci* **2017,** *18*, 1545.
13. Fakhari, A.; Berkland, C. Applications and emerging trends of hyaluronic acid in tissue engineering, as a dermal filler and in osteoarthritis treatment. *Acta Biomater* **2013,** *9*, 7081-92.
14. Özçelik, H.; Vrana, N. E.; Gudima, A.; Riabov, V.; Gratchev, A.; Haikel, Y.; Metz-Boutigue, M. H.; Carradò, A.; Faerber, J.; Roland, T.; Klüter, H.; Kzhyshkowska, J.; Schaaf, P.; Lavalle, P. Harnessing the multifunctionality in nature: a bioactive agent release system with self-antimicrobial and immunomodulatory properties. *Adv Healthc Mater* **2015,** *4*, 2026-36.
15. Mutschler, A.; Tallet, L.; Rabineau, M.; Dollinger, C.; Metz-Boutigue, M.-H.; Schneider, F.; Senger, B.; Vrana, N. E.; Schaaf, P.; Lavalle, P. Unexpected Bactericidal Activity of Poly(arginine)/Hyaluronan Nanolayered Coatings. *Chem Mater* **2016,** *28*, 8700-8709.
16. Mutschler, A.; Betscha, C.; Ball, V.; Senger, B.; Vrana, N. E.; Boulmedais, F.; Schroder, A.; Schaaf, P.; Lavalle, P. Nature of the Polyanion Governs the Antimicrobial Properties of Poly(arginine)/Polyanion Multilayer Films. *Chem Mater* **2017,** *29*, 3195-3201.
17. Gribova, V.; Boulmedais, F.; Dupret-Bories, A.; Calligaro, C.; Senger, B.; Vrana, N. E.; Lavalle, P. Polyanionic Hydrogels as Reservoirs for Polycationic Antibiotic Substitutes Providing Prolonged Antibacterial Activity. *ACS Appl Mater Interfaces* **2020,** *12*, 19258-19267.

18. Al-Sibani, M.; Al-Harrasi, A.; Neubert, R. H. Study of the effect of mixing approach on cross-linking efficiency of hyaluronic acid-based hydrogel cross-linked with 1,4-butanediol diglycidyl ether. *Eur J Pharm Sci* **2016,** *91*, 131-7.
19. Fuchs, S. M.; Raines, R. T. Pathway for polyarginine entry into mammalian cells. *Biochemistry* **2004,** *43*, 2438-44.
20. Xing, H.; Lu, M.; Yang, T.; Liu, H.; Sun, Y.; Zhao, X.; Xu, H.; Yang, L.; Ding, P. Structure-function relationships of nonviral gene vectors: Lessons from antimicrobial polymers. *Acta Biomater* **2019,** *86*, 15-40.
21. Chen, Y.; Gao, D. Y.; Huang, L. In vivo delivery of miRNAs for cancer therapy: challenges and strategies. *Adv Drug Deliv Rev* **2015,** *81*, 128-41.
22. Chakraborty, C.; Sharma, A. R.; Sharma, G.; Lee, S.-S. Therapeutic advances of miRNAs: A preclinical and clinical update. *J Adv Res* **2021,** *28*, 127-138.
23. Carthew, J.; Donderwinkel, I.; Shrestha, S.; Truong, V. X.; Forsythe, J. S.; Frith, J. E. In situ miRNA delivery from a hydrogel promotes osteogenesis of encapsulated mesenchymal stromal cells. *Acta Biomater* **2020,** *101*, 249-261.
24. Saleh, B.; Dhaliwal, H. K.; Portillo-Lara, R.; Shirzaei Sani, E.; Abdi, R.; Amiji, M. M.; Annabi, N. Local Immunomodulation Using an Adhesive Hydrogel Loaded with miRNA-Laden Nanoparticles Promotes Wound Healing. *Small* **2019,** *15*, 1902232.
25. Zhou, Y. L.; Yang, Q. Q.; Yan, Y. Y.; Zhu, C.; Zhang, L.; Tang, J. B. Localized delivery of miRNAs targets cyclooxygenases and reduces flexor tendon adhesions. *Acta Biomater* **2018,** *70*, 237-248.
26. Wang, L. L.; Liu, Y.; Chung, J. J.; Wang, T.; Gaffey, A. C.; Lu, M.; Cavanaugh, C. A.; Zhou, S.; Kanade, R.; Atluri, P.; Morrisey, E. E.; Burdick, J. A. Sustained miRNA delivery from an injectable hydrogel promotes cardiomyocyte proliferation and functional regeneration after ischaemic injury. *Nat Biomed* **2017,** *1*, 983-992.
27. Sridharan, R.; Cameron, A. R.; Kelly, D. J.; Kearney, C. J.; O'Brien, F. J. Biomaterial based modulation of macrophage polarization: a review and suggested design principles. *Mater Today* **2015,** *18*, 313-325.
28. Hickey, M. J. Role of inducible nitric oxide synthase in the regulation of leucocyte recruitment. *Clin Sci* **2000,** *100*, 1-12.
29. Mescher, A. L. Macrophages and fibroblasts during inflammation and tissue repair in models of organ regeneration. *Regeneration (Oxf)* **2017,** *4*, 39-53.